

# Co-Generation of C<sub>2</sub> Hydrocarbons and Synthesis Gases from Methane and Carbon Dioxide: a Thermodynamic Analysis

Istadi<sup>1)</sup>, Nor Aishah Saidina Amin\*

*Chemical Reaction Engineering Group (CREG), Faculty of Chemical and Natural Resources Engineering, Universiti Teknologi Malaysia, UTM Skudai, Johor, 81310 Malaysia*

[Manuscript received August 01, 2005; revised September 08, 2005]

**Abstract:** This paper deals with thermodynamic chemical equilibrium analysis using the method of direct minimization of Gibbs free energy for all possible CH<sub>4</sub> and CO<sub>2</sub> reactions. The effects of CO<sub>2</sub>/CH<sub>4</sub> feed ratio, reaction temperature, and system pressure on equilibrium composition, conversion, selectivity and yield were studied. In addition, carbon and no carbon formation regions were also considered at various reaction temperatures and CO<sub>2</sub>/CH<sub>4</sub> feed ratios in the reaction system at equilibrium. It was found that the reaction temperature above 1100 K and CO<sub>2</sub>/CH<sub>4</sub> ratio=1 were favourable for synthesis gas production with H<sub>2</sub>/CO ratio unity, while carbon dioxide oxidative coupling of methane (CO<sub>2</sub> OCM) reaction to produce ethane and ethylene is less favourable thermodynamically. Numerical results indicated that the no carbon formation region was at temperatures above 1000 K and CO<sub>2</sub>/CH<sub>4</sub> ratio larger than 1.

**Key words:** thermodynamic chemical equilibrium, co-generation, synthesis gas, C<sub>2</sub> hydrocarbons, Gibbs free energy, CH<sub>4</sub>, CO<sub>2</sub>, carbon

## 1. Introduction

The simultaneous utilization of CH<sub>4</sub> and CO<sub>2</sub> for conversion to important chemicals provides several advantages from the environmental and energy perspectives. Natural gas is a fuel consisting of methane, ethane, carbon dioxide, H<sub>2</sub>S, and trace amounts of other compounds. It is highly desirable to utilize and to convert both methane and carbon dioxide, two typical components in acidic natural gas, into higher value-added chemicals and also liquid fuels [3] without having to separate the carbon dioxide first. The composition of natural gas varies widely from location to location. For example, the CO<sub>2</sub>/CH<sub>4</sub> ratio of natural gas in Natuna's [1] and Arun's [2] fields are 71/28 and 15/75, respectively.

The co-generation of synthesis gas and C<sub>2</sub> hydro-

carbons from CH<sub>4</sub> and CO<sub>2</sub> is important in the utilization of CO<sub>2</sub>-contented natural gas. The process yields lower H<sub>2</sub>/CO molar ratio synthesis gas and light hydrocarbons (C<sub>2</sub> hydrocarbons). The synthesis gas (H<sub>2</sub> and CO) can be converted to liquid fuels by the Fischer-Tropsch process and also to various value-added chemicals, especially methanol and gasoline *via* the methanol-to-gasoline (MTG) process. The synthesis gas is also the main source of hydrogen for refinery processes and ammonia synthesis. The use of CO<sub>2</sub> as an oxidant for the selective oxidation of methane may also be beneficial, because it is expected that the replacement of O<sub>2</sub> with CO<sub>2</sub> inhibits the gas-phase non-selective oxidation and thus increases the selectivity to higher hydrocarbons. Previously, the thermodynamic calculation on equilibrium conversion of CH<sub>4</sub> to C<sub>2</sub> hydrocarbons (C<sub>2</sub>H<sub>6</sub>

\* Corresponding author. Tel. +607-5535588; Fax. +607-5581463; E-mail: noraishah@fkkksa.utm.my.

1) Permanent address: Chemical Reaction Engineering & Catalysis Group, Dept. of Chemical Engineering, Diponegoro University, Semarang, Indonesia. E-mail: istadi@tekim.ft.undip.ac.id

and  $C_2H_4$ ) showed that the equilibrium conversion increased with rising temperature or  $CO_2/CH_4$  feed ratio [4]. However, comprehensive thermodynamic equilibrium studies on the co-generation of synthesis gas and  $C_2$  hydrocarbons from methane and carbon dioxide have not been conducted previously. Accordingly, the results of thermodynamic studies can identify the constraints placed in a reacting system and can provide the recommendation of suitable operating conditions for the catalytic reacting system theoretically.

The study on thermodynamic equilibrium composition has been used in investigating the feasibility of many types of reaction. Vasudeva *et al.* [5] computed equilibrium compositions for steam reforming of ethanol to examine the viability of the process. Similarly, Chan *et al.* [6] examined the thermodynamic equilibrium compositions for simultaneous partial oxidation and steam reforming of natural gas. Global reaction balances and chemical equilibrium of steam reforming and partial oxidation to produce hydrogen were studied by Lutz *et al.* [7,8] for the same objective. Thermodynamic chemical equilibrium on methane pyrolysis process were also reported by Guéret *et al.* [9] using the direct Gibbs free energy minimization. Similar method was also performed by Lwin *et al.* [10] on the hydrogen production from steam-methanol reforming. The method of the direct minimization of Gibbs free energy of a system was used by Chan *et al.* [6,9,11] for solving equilibrium thermodynamic analysis of supercritical water gasification of biomass, steam reforming of ethanol for hydrogen production, and methane pyrolysis, respectively. Meanwhile, the minimization of Gibbs free energy using Lagrange's multiplier was implemented by Douvartzides *et al.* [6,12–14] for solving thermodynamic equilibrium analysis of solid oxide fuel cells, natural-gas fuel processing for fuel cell applications, autothermal methanol reformer, and catalytic combustion of methane, respectively.

The main objective of this paper is to perform a thermodynamic chemical equilibrium analysis of all possible  $CH_4$  and  $CO_2$  reactions in the co-generation of  $C_2$  hydrocarbons and synthesis gas. In this analysis, the effect of various conditions, *i.e.* temperature,  $CO_2/CH_4$  feed ratio and system pressure, on chemical equilibrium are discussed. In addition, the effects of  $CO_2/CH_4$  feed ratio and temperature on carbon formation in the reaction system at equilibrium are also investigated. Through the thermodynamic equilibrium analysis, the feasibility of reactions in a reacting system can be addressed.

## 2. Technique for calculation of thermodynamic chemical equilibrium

There are two common ways to express the chemical equilibrium. One is based on equilibrium constants ( $K$ ), while the other is based on the minimization of Gibbs free energy [15]. There are two alternative methods for solving the minimization of the Gibbs free energy, *i.e.* direct minimization and the use of Lagrangian multiplier. The direct minimization of Gibbs free energy was reported to be effective for complicated chemical equilibrium problems. The method, which is a default method in Chemkin, is used to solve the chemical equilibrium system at various temperatures,  $CO_2/CH_4$  ratios, or system pressures without requiring detailed information about the homogeneous or heterogeneous reaction rate.

In this paper, the global and chemical equilibrium analysis of reactions between  $CH_4$  and  $CO_2$ , where  $CH_4$ ,  $CO_2$ ,  $CO$ ,  $H_2$ ,  $C_2H_4$ ,  $C_2H_6$  and  $H_2O$  exist in the equilibrium system, are considered.  $CH_4$  and  $CO_2$  are stated as the reactants, while  $CO$ ,  $H_2$ ,  $C_2H_4$ ,  $C_2H_6$  and  $H_2O$  are defined as products. The possible main reactions between  $CH_4$  and  $CO_2$  to produce the equilibrium products are listed in Table 1, identified as Reactions (1)–(5). The chemical equilibrium calculations were carried out using Chemkin Interface for Stanjan (Chemkin Collection R3.7.1) to compute the chemical composition at specified temperature and pressure. The practical use of the calculation method in Chemkin requires the following parameters: (a) the substances likely to be present at equilibrium, (b) the elements information within the system, and (c) initial compositions of the chemical species. The thermodynamic properties data for equilibrium calculation of the system are available readily in the Chemkin software. Nevertheless, the chemical compositions predicted by the equilibrium analysis are still theoretical upper limits for the process and the optimal conditions may change in practice.

**Table 1. The possible reactions of  $CH_4$  and  $CO_2$  considered in the thermodynamic analysis**

Reaction No	Reaction schemes	$\Delta H_{298}^\circ$ / (kJ/mol)
(1)	$CH_4 + CO_2 \rightleftharpoons 2CO + 2H_2$	247
(2)	$CO_2 + H_2 \rightleftharpoons CO + H_2O$	41
(3)	$2CH_4 + CO_2 \rightleftharpoons C_2H_6 + CO + H_2O$	106
(4)	$2CH_4 + 2CO_2 \rightleftharpoons C_2H_4 + 2CO + 2H_2O$	284
(5)	$C_2H_6 \rightleftharpoons C_2H_4 + 2H_2$	136

Pertaining to direct Gibbs free energy minimization method used in the Chemkin, the basic equations for the chemical equilibrium calculation is considered. Consider an initial system of  $N_i$  mole of each of the  $I$  chemical species. The total Gibbs free energy  $G$  of the system is expressed as [15]:

$$G = \sum_{i=1}^I N_i \bar{g}_i = \sum_{i=1}^I N_i [(\bar{g}_i - g_i^o) + g_i^o] \quad (1)$$

where  $\bar{g}_i$  is the partial molar Gibbs free energy of the  $i$ th species in solution at operating conditions,  $g_i^o$  is the Gibbs free energy of the pure  $i$ th species at standard conditions, and  $N_i$  is the number of moles of each species  $i$  in the system. Using the relation [15]:

$$\bar{g}_i - g_i^o = RT \ln \frac{\hat{f}_i}{f_i^o} \quad (2)$$

where  $\hat{f}_i$  is the fugacity of species  $i$  in solution at operating conditions, and  $f_i^o$  is the fugacity of pure species  $i$  in its standard state, the Equation (1) can be written as:

$$G = \sum_{i=1}^I N_i \left[ g_i^o + RT \ln \frac{\hat{f}_i}{f_i^o} \right] \quad (3)$$

If all the species are in the gaseous state and letting the reaction system pressure to be  $P$ , we can write [15]:

$$\frac{\hat{f}_i}{y_i P} = \hat{\phi}_i \quad \text{and} \quad \hat{f}_i = \hat{\phi}_i y_i P = \hat{\phi}_i \frac{N_i}{N} P \quad (4)$$

Meanwhile, the equilibrium constant ( $K$ ) of the reactions can be predicted by the following Equation:

$$\ln K = \frac{-\Delta G_T^o}{RT} \quad (9)$$

The equilibrium conversion, selectivity and yield were calculated based on the initial and equilibrium compositions resulted by Chemkin. The molar flow rate of the outlet reactor can be determined from the mass balance by utilizing the information from Chemkin results. The conversions of  $\text{CH}_4$  and  $\text{CO}_2$  are calculated by Equation (10).

$$X_i = \frac{n_{i,\text{in}} - n_{i,\text{out}}}{n_{i,\text{in}}} \times 100\% \quad (10)$$

where  $N$  is total number of moles in the reaction mixture including the unreacted species;  $\hat{\phi}_i$  is the fugacity coefficient of the  $i$ th species in solution, and  $y_i$  is mole fraction of the  $i$ th species. Since standard state is taken as pure ideal gas state at 1 atm,  $f_i^o$  equals to 1 [10,15]. At low pressure and/or high temperature, the system can be considered to be ideal gas mixtures or ideal solutions in which  $\hat{\phi}_i=1$ , Equation (3) becomes:

$$G = \sum_{i=1}^I N_i \left[ g_i^o + RT \ln \frac{N_i}{N} + RT \ln P \right] \quad (5)$$

$$\text{or} \quad G = \sum_{i=1}^I N_i RT \left[ \frac{g_i^o}{RT} + \ln y_i + \ln P \right] \quad (6)$$

where  $R$  is the universal gas constant, and  $y_i$  is the mole fraction of the  $i$ th species.

The equilibrium solution at a given temperature and pressure is the distribution of  $N_i$  or  $y_i$  that minimizes the system Gibbs function,  $G$ , subject to the elemental mass balance and non-negative  $N_i$  constraints. The elemental mass balance constraints are:

$$\sum_{i=1}^I n_{ji} N_i = b_j \quad j = 1, \dots, J \quad (7)$$

where  $n_{ji}$  is the number of the  $j$ th atoms that appear in the  $i$ th molecule,  $b_j$  is the total population in moles of the  $j$ th atom in the system, and  $J$  is the total number of different elements/atoms that are present in the system.

The standard Gibbs free energy changes ( $\Delta G_T^o$ ) at system temperature  $T$  used in analysis of the reactions is calculated by the following equation [15]:

$$\frac{\Delta G_T^o}{RT} = \frac{\Delta G_0^o - \Delta H_0^o}{RT_0} + \frac{\Delta H_0^o}{RT} + \frac{1}{T} \int_{T_0}^T \frac{\Delta C_p^o}{R} dT - \int_{T_0}^T \frac{\Delta C_p^o}{RT} dT \quad (8)$$

where  $i$  corresponds to  $\text{CH}_4$  and  $\text{CO}_2$  and  $n_i$  is mol of species  $i$ . The selectivities of  $\text{C}_2\text{H}_6$ ,  $\text{C}_2\text{H}_4$ , and  $\text{CO}$  can be determined by Equation (11), while  $\text{H}_2$  selectivity is calculated by Equation (12).

$$S_i = \frac{n_{i,\text{out}} n_{c,i}}{(n_{\text{CH}_4,\text{in}} - n_{\text{CH}_4,\text{out}}) + (n_{\text{CO}_2,\text{in}} - n_{\text{CO}_2,\text{out}})} \times 100\% \quad (11)$$

$$S_{\text{H}_2} = \frac{n_{\text{H}_2,\text{out}}}{2(n_{\text{CH}_4,\text{in}} - n_{\text{CH}_4,\text{out}})} \times 100\% \quad (12)$$

where  $i$  denotes  $\text{C}_2\text{H}_6$ ,  $\text{C}_2\text{H}_4$ , and  $\text{CO}$ , and  $n_c$  is the number of carbon atom in the corresponding species. The yields of  $\text{C}_2\text{H}_6$ ,  $\text{C}_2\text{H}_4$ , and  $\text{CO}$  are calculated by

Equation (13), while  $H_2$  yield can be determined by Equation (14).

$$Y_i = \frac{n_{i,out}n_{c,i}}{(n_{CH_4,in} + n_{CO_2,in})} \times 100\% \quad (13)$$

$$Y_{H_2} = \frac{n_{H_2,out}}{2n_{CH_4,in}} \times 100\% \quad (14)$$

where  $i$  is  $C_2H_6$ ,  $C_2H_4$ , and  $CO$ . The ranges of conditions under which carbon will form in the system are presented as carbon and non-carbon region as function of  $CO_2/CH_4$  feed ratio and temperature. The curve is plotted by determining the points corresponding to the first disappearance of carbon as the temperature is increased for a fixed feed ratio.

### 3. Results and discussion

#### 3.1. Standard Gibbs free energy change analysis of $CH_4$ and $CO_2$ reactions

The feasibility of the reactions (Reactions (1–5)) can be studied from the standard Gibbs free energy change of the reactions defined as the difference between Gibbs free energy change of the products and reactants (weighted by their stoichiometric coefficients) at standard state (pure substance, 1 atm), and system temperature [15]. The standard Gibbs free energy changes ( $\Delta G_T^\circ$ ) of the reactions tabulated in Table 2 are calculated based on Equation (8), while the equilibrium constants of the reactions listed in Table 3 are calculated from Equation (9).

**Table 2. Standard Gibbs free energy change ( $\Delta G_T^\circ$ ) of the reactions at various temperature**

Reaction	$\Delta G_T^\circ / (kJ/mol)$									
	298 K	373 K	473 K	573 K	673 K	773 K	873 K	973 K	1073 K	1173 K
Reaction (1)	170.48	150.89	123.99	96.58	68.84	40.92	12.93	−15.09	−43.08	−71.02
Reaction (2)	79.08	69.97	58.25	47.07	36.45	26.39	16.88	7.90	−0.57	−8.54
Reaction (3)	97.68	95.43	92.31	89.13	85.91	82.66	79.39	76.12	72.85	69.57
Reaction (4)	226.62	212.01	192.18	172.16	152.06	131.95	111.86	91.83	71.87	51.98
Reaction (5)	100.32	90.85	77.20	62.67	47.48	31.76	15.62	−0.87	−17.65	−34.67

**Table 3. Equilibrium constant ( $K$  value) of the reactions at various temperature**

Reaction	Equilibrium constant ( $K=\exp(-\Delta G_T^\circ/\text{RT})$ )								
	298 K	473 K	573 K	673 K	773 K	873 K	973 K	1073 K	1173 K
Reaction (1)	1.31E-30	2.02E-14	1.57E-9	4.54E-6	1.72E-3	1.68E-1	6.46	1.252E2	1.454E3
Reaction (2)	1.38E-14	3.69E-7	5.11E-5	1.48E-3	1.65E-2	9.77E-2	0.38	1.07	2.40
Reaction (3)	7.54E-18	6.39E-11	7.50E-9	2.15E-7	2.60E-6	1.78E-5	8.19E-5	2.84E-4	7.98E-4
Reaction (4)	1.89E-40	5.98E-22	2.02E-16	1.58E-12	1.21E-9	2.03E-7	1.18E-5	3.17E-4	4.84E-3
Reaction (5)	2.61E-18	2.98E-9	1.94E-6	2.06E-4	7.14E-3	0.12	1.11	7.23	3.499E1

In general, the chemical reactions can be reversed, at which the final equilibrium composition is governed by the minimum Gibbs free energy. The total Gibbs free energy of a closed system at constant  $T$  and  $P$  decreases during the irreversible reactions process. The condition for equilibrium is reached when Gibbs free energy attains its minimum value or in other word Gibbs free energy change equal to zero [15]. Thermodynamically, if the Gibbs free energy change ( $\Delta G_T^\circ$ ) at certain temperature decreases to a high negative value or consequently the equilibrium constant ( $K$ ) attains a high value, the reactions are favourable (the reaction shifts to the product side). On the contrary, if the Gibbs free energy change ( $\Delta G_T^\circ$ ) at certain temperature increases to a high positive value or the equilib-

rium constant ( $K$ ) tends to a lower value, the reaction is not favourable (the reaction shifts to the reactant side) [15].

From Tables 2 and 3, it can be deduced that the  $CH_4$ - $CO_2$  reaction to form synthesis gas ( $H_2$  and  $CO$ ) is the most favourable reaction (Reaction 1), particularly at high temperature ( $>1000$  K). In general, the reaction is typically accompanied by the simultaneous occurrence of Reaction 2. The high positive value of  $\Delta G_T^\circ$  at all temperature ranges reveals that the  $CO_2$  OCM reaction (Reactions (3) and (4)) are less feasible at equilibrium thermodynamically. During the  $CO_2$  OCM reaction, dehydrogenation reaction (Reaction (5)) also occurs simultaneously. From Tables 2 and 3, it is shown that the Reaction 5 is favourable

at high temperature rather than  $\text{CO}_2$  OCM reaction, and thus reduces the mole fraction of ethane at equilibrium.

### 3.2. Effect of temperature on equilibrium mole fraction, conversion, selectivity and yield

Thermodynamically, effect of temperature on the equilibrium composition can be studied from the following relations [15]:

$$\frac{d(\Delta G^\circ/RT)}{dT} = \frac{-\Delta H^\circ}{RT^2} \quad (15)$$

or

$$\frac{d \ln K}{dT} = \frac{\Delta H^\circ}{RT^2} \quad (16)$$

Since the reactions considered are all endothermic, the standard Gibbs free energy change ( $\Delta G_T^\circ$ ) decreases and the equilibrium constant ( $K$ ) increases with increasing temperature and therefore shifts the reaction to the product side [15].

The effects of temperature on the chemical equilibrium compositions for methane-carbon dioxide reactions are shown in Figures 1(a)–(c) for  $\text{CO}_2/\text{CH}_4$  feed ratios 0.5, 1, and 2, respectively. In Figure 1(a), a considerable increase of  $\text{C}_2\text{H}_4$  mole fraction is exhibited particularly at higher reaction temperature due to the lower  $\Delta G_T^\circ$  in Reaction (4) ( $\text{C}_2\text{H}_6$  production reaction) as compared to Reaction (3) ( $\text{C}_2\text{H}_4$  production reaction). The trend can also be contributed to

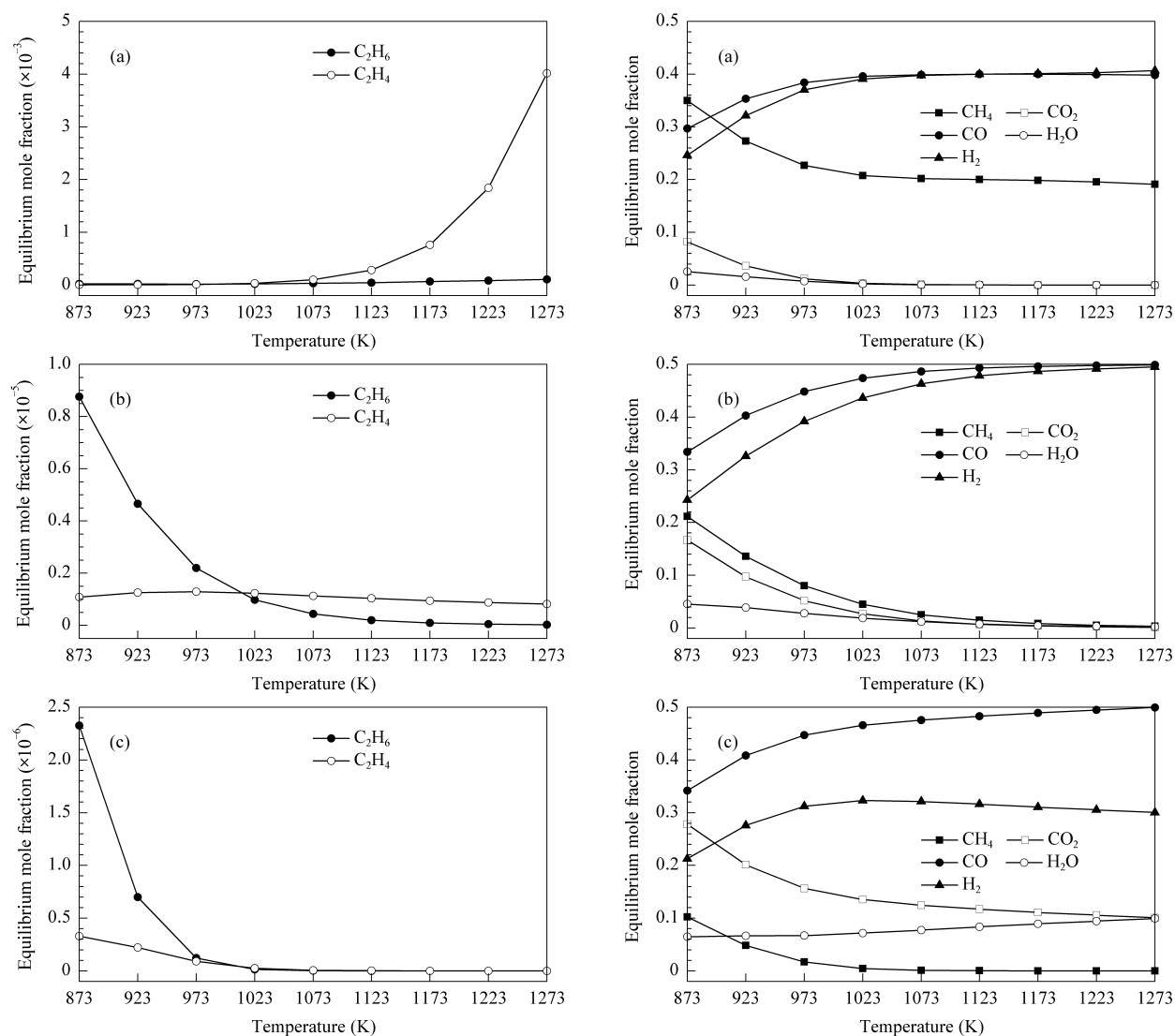


Figure 1. Effect of temperature on equilibrium mole fractions at 1 atm

(a)  $\text{CO}_2/\text{CH}_4 = 1/2$ , (b)  $\text{CO}_2/\text{CH}_4 = 1$ , (c)  $\text{CO}_2/\text{CH}_4 = 2$

more hydrogen atom content within the equilibrium system. The  $\text{H}_2$  and  $\text{CO}$  compositions at equilibrium increase with temperature. For higher  $\text{CO}_2/\text{CH}_4$  feed ratio, both  $\text{C}_2\text{H}_4$  and  $\text{C}_2\text{H}_6$  mole fractions decrease as temperature increases. The trends reveal that there is a correlation between reaction temperature and contribution of H atom from methane at equilibrium system leading to a significant effect on the ethylene and ethane products formation. Higher reaction temperature and lower  $\text{CO}_2/\text{CH}_4$  feed ratio increase the  $\text{C}_2\text{H}_6$  and  $\text{C}_2\text{H}_4$  compositions at equilibrium conditions. The results in Figure 1 reveal that  $\text{H}_2$  mole fraction is smaller than that of  $\text{CO}$  at all  $\text{CO}_2/\text{CH}_4$  feed ratio and the effect is more pronounced for higher  $\text{CO}_2/\text{CH}_4$  feed ratio. The  $\text{H}_2$  can react with  $\text{CO}_2$  to form less  $\text{H}_2\text{O}$  and  $\text{CO}$  in Reaction (2) and the trend is consistent with the results for catalytic carbon dioxide

reforming of methane reaction [16].

Meanwhile, Figures 2(a) and 2(b) present the effect of temperature on the  $\text{CH}_4$  and  $\text{CO}_2$  equilibrium conversion at  $\text{CO}_2/\text{CH}_4$  feed ratio being 1 and 2, respectively, while the pressure is kept constant at 1 atm. At  $\text{CO}_2/\text{CH}_4$  ratio 1,  $\text{CH}_4$  conversion is lower than  $\text{CO}_2$ , since the  $\text{CO}_2$  can react with  $\text{H}_2$  to form  $\text{CO}$  and water in the Reaction (2). The reverse water gas shift reaction (Reaction (2)) phenomenon is particularly enhanced with increasing  $\text{CO}_2/\text{CH}_4$  feed ratio as indicated by the increasing water equilibrium mole fraction at higher temperature in Figure 1(c). The distinct trend in the conversion is exhibited by the  $\text{CO}_2/\text{CH}_4$  feed ratio 2 (Figure 2(b)), where  $\text{CH}_4$  conversion is higher than that of  $\text{CO}_2$  since  $\text{CH}_4$  is the limiting reactant.

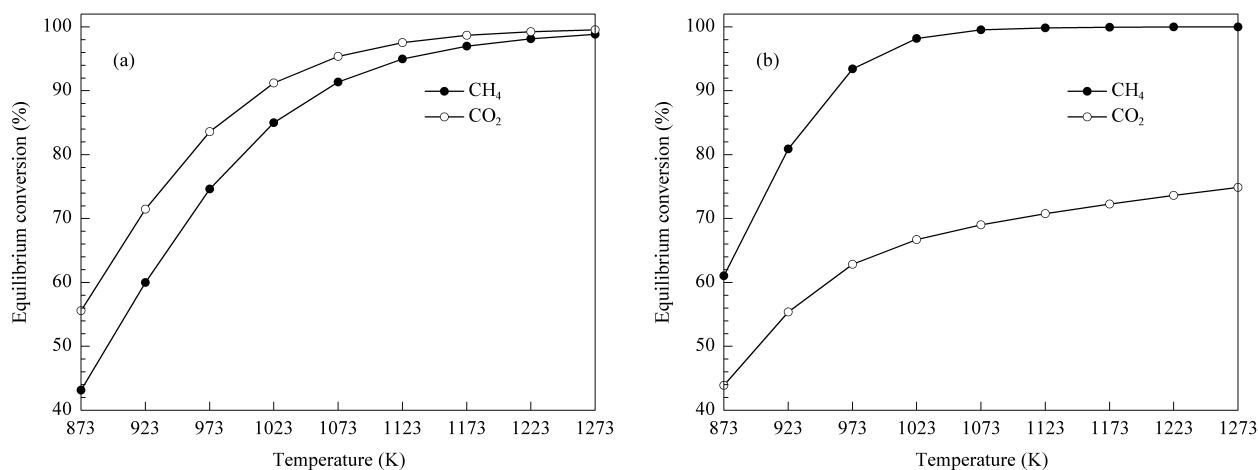


**Figure 2.** Effect of temperature on equilibrium conversions of  $\text{CH}_4$  and  $\text{CO}_2$  at 1 atm

(a)  $\text{CO}_2/\text{CH}_4=1$ , (b)  $\text{CO}_2/\text{CH}_4=2$

Hydrogen and carbon monoxide are potential products for  $\text{CH}_4\text{-CO}_2$  reaction equilibrium system owing to their good selectivity and yield at higher temperature as exhibited in Figures 3 and 4, respectively. Considerable improvement in the hydrogen selectivity is obtained as the temperature increased from 873 K up to 1000 K as presented in Figures 3(a) and 3(b) at  $\text{CO}_2/\text{CH}_4$  feed ratio being 1 and 2, respectively. Similar trends are observed in Figures 4(a) and 4(b) with respect to hydrogen yield at  $\text{CO}_2/\text{CH}_4$  feed ratio of 1 and 2, respectively. However, the hydrogen selectivity and yield decrease at reactor temperature higher than 1000 K, particularly for  $\text{CO}_2/\text{CH}_4$  feed ratio being 2 as exhibited in Figures 3(b) and 4(b). The  $\text{H}_2$  reacts with  $\text{CO}_2$  to produce  $\text{CO}$  and water in Reaction (2) at the conditions due to high  $\text{CO}_2/\text{CH}_4$

ratio in the feed. The Reaction (2) is favoured at high temperature as evident by the  $\Delta G_T^\circ$  value presented in Tables 2 and 3. Indeed, the  $\text{CO}$  yield exceeds the  $\text{H}_2$  yield at temperature above 1000 K as revealed in Figure 4(b).

Pertaining to equilibrium selectivity and yield of  $\text{C}_2\text{H}_6$  and  $\text{C}_2\text{H}_4$ , the  $\text{C}_2\text{H}_6$  formation is more favourable than  $\text{C}_2\text{H}_4$  at temperature lower than 1000 K as shown in Figures 3 and 4, respectively. This trend is confirmed by higher  $\Delta G_T^\circ$  value for the  $\text{CO}_2$  OCM reaction to form  $\text{C}_2\text{H}_6$  (Reaction (3)) than that of  $\text{C}_2\text{H}_4$  (Reaction (4)) at the temperature below 1000 K as exhibited in Table 2. The equilibrium selectivity and yield of  $\text{C}_2\text{H}_4$  surpass that of  $\text{C}_2\text{H}_6$  at temperature higher than 1000 K as demonstrated in Figures 3(a) and 4(a) at  $\text{CO}_2/\text{CH}_4$  feed ratio being 1, which

can be confirmed by lower  $\Delta G_T^\circ$  value for the  $\text{CO}_2$  OCM reaction to form  $\text{C}_2\text{H}_4$  (Reaction (4)) compared to  $\text{C}_2\text{H}_6$  (Reaction (3)) at temperature above 1000 K as shown in Table 2. Additionally, the  $\text{C}_2\text{H}_6$  may react with  $\text{CO}_2$  to form  $\text{C}_2\text{H}_4$  at high temperature ow-

ing to  $\text{CO}_2$  dehydrogenation reaction. However, the trend for the equilibrium selectivity and yield of  $\text{C}_2\text{H}_4$  and  $\text{C}_2\text{H}_6$  at temperature above 1000 K is different for  $\text{CO}_2/\text{CH}_4$  ratio 2 as exhibited in Figures 3(b) and 4(b), respectively.

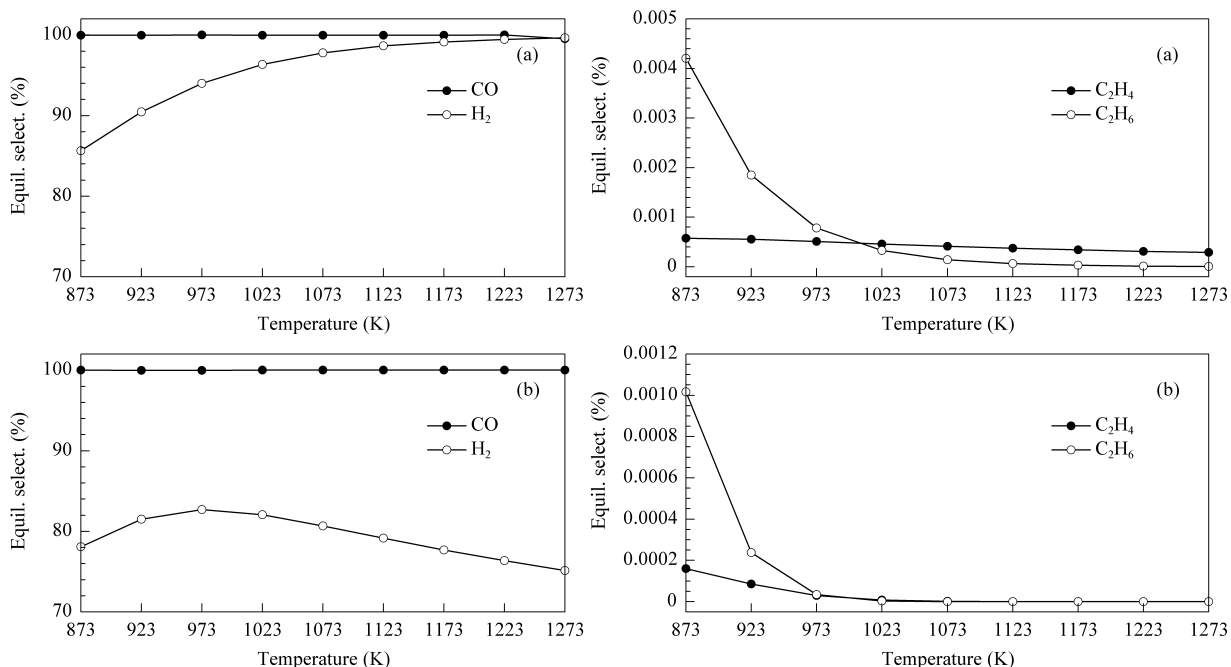


**Figure 3.** Effect of temperature on equilibrium selectivities of  $\text{H}_2$ ,  $\text{CO}$ ,  $\text{C}_2\text{H}_6$  and  $\text{C}_2\text{H}_4$  products at 1 atm (a)  $\text{CO}_2/\text{CH}_4=1$ , (b)  $\text{CO}_2/\text{CH}_4=2$

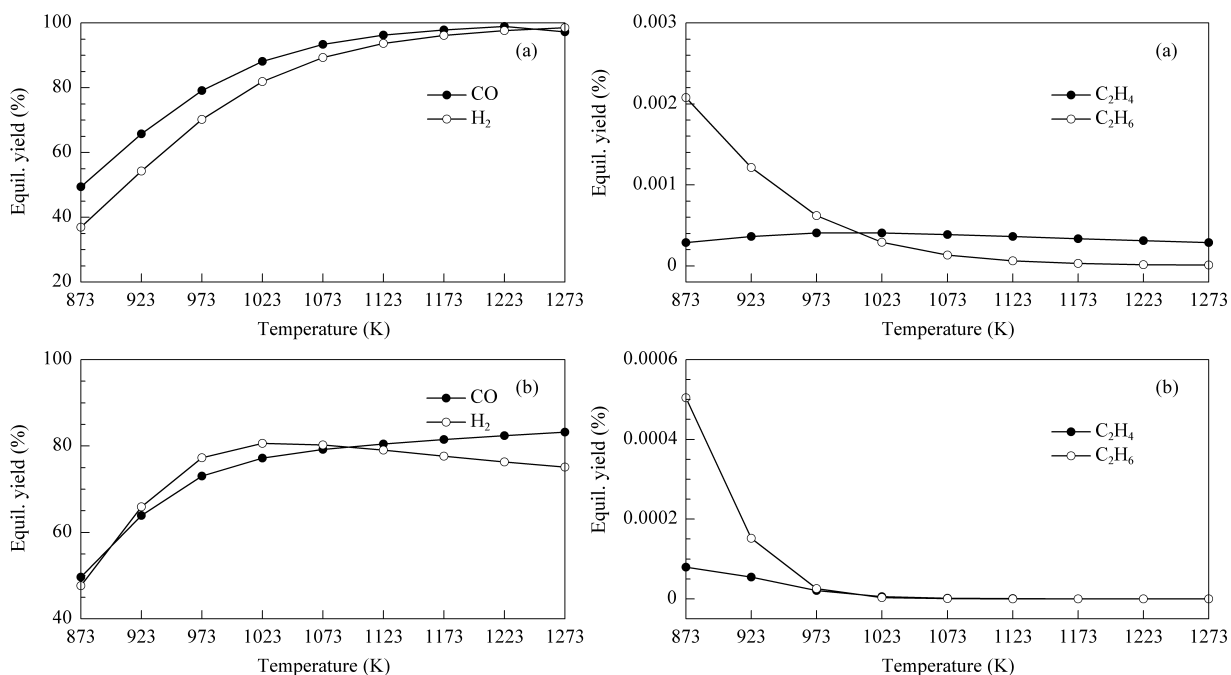


**Figure 4.** Effect of temperature on equilibrium yields of  $\text{H}_2$ ,  $\text{CO}$ ,  $\text{C}_2\text{H}_6$  and  $\text{C}_2\text{H}_4$  products at 1 atm (a)  $\text{CO}_2/\text{CH}_4=1$ , (b)  $\text{CO}_2/\text{CH}_4=2$

### 3.3. Effect of CO<sub>2</sub>/CH<sub>4</sub> feed ratio on equilibrium mole fraction, conversion, selectivity and yield

In this section the chemical equilibrium compositions are predicted for different CO<sub>2</sub>/CH<sub>4</sub> feed ratios presented in Table 4 at 1123 K and 1 atm. From the Table, as the CO<sub>2</sub>/CH<sub>4</sub> feed ratio increases, the equilibrium mole fractions for C<sub>2</sub>H<sub>6</sub> and C<sub>2</sub>H<sub>4</sub> decrease as there is less CH<sub>4</sub>, and therefore less H atom in the system. The C<sub>2</sub>H<sub>6</sub> mole fraction is less than C<sub>2</sub>H<sub>4</sub> at higher CO<sub>2</sub>/CH<sub>4</sub> feed ratio due to the reaction of

C<sub>2</sub>H<sub>6</sub> with CO<sub>2</sub> to form C<sub>2</sub>H<sub>4</sub> in CO<sub>2</sub> dehydrogenation reaction. However, H<sub>2</sub> and CO mole fractions increase with CO<sub>2</sub>/CH<sub>4</sub> feed ratio. Both values achieve their maximum at CO<sub>2</sub>/CH<sub>4</sub> feed ratio being 1. The increment may be due to the CO<sub>2</sub> role as the limiting reactant, which in turn improves oxidation strength of CO<sub>2</sub> towards methane at equilibrium condition. Increasing CO<sub>2</sub>/CH<sub>4</sub> feed ratio above 1 leads to decrement of both H<sub>2</sub> and CO at equilibrium which may be attributed to Reaction (2) being favourable at high temperature as exhibited in Tables 2 and 3.

**Table 4. Effect of CO<sub>2</sub>/CH<sub>4</sub> feed ratio on equilibrium performances at 1123 K and 1 atm**

CO <sub>2</sub> /CH <sub>4</sub> feed ratio	Mole fraction							X/%		S/%				Y/%			
	CH <sub>4</sub>	CO <sub>2</sub>	H <sub>2</sub>	CO	C <sub>2</sub> H <sub>6</sub>	C <sub>2</sub> H <sub>4</sub>	H <sub>2</sub> O	CH <sub>4</sub>	CO <sub>2</sub>	H <sub>2</sub>	CO	C <sub>2</sub> H <sub>6</sub>	C <sub>2</sub> H <sub>4</sub>	H <sub>2</sub>	CO	C <sub>2</sub> H <sub>6</sub>	C <sub>2</sub> H <sub>4</sub>
Pure CH <sub>4</sub>	0.82	—	0.12	—	2.72E-3	5.69E-2	—	13.05	—	48.74	—	4.42	92.44	6.36	—	0.57	12.07
0.25	0.42	2.94E-5	0.29	0.29	2.87E-4	2.42E-3	3.3E-5	26.33	99.98	96.58	99.10	0.20	1.65	25.43	40.69	0.08	0.68
0.33	0.33	6.86E-5	0.34	0.33	1.52E-4	1.11E-3	7.5E-5	33.89	99.97	99.08	99.14	0.09	0.77	33.58	49.98	0.05	0.39
0.51	0.19	2.47E-4	0.40	0.40	4.37E-5	2.65E-4	2.7E-4	51.02	99.91	99.77	99.83	0.02	0.15	50.90	67.41	0.02	0.10
0.74	8.45E-2	9.38E-4	0.46	0.46	7.33E-6	3.93E-5	1.0E-3	73.44	99.68	99.80	99.98	3.1E-3	0.02	73.30	84.57	2.6E-3	0.02
1.00	1.44E-2	7.02E-3	0.48	0.49	2.03E-7	1.04E-6	7.4E-3	94.98	97.56	98.64	99.99	1.0E-4	4.0E-4	93.68	96.27	1.0E-4	4.0E-4
1.96	3.89E-4	0.11	0.32	0.48	2.2E-10	1.68E-9	8.2E-2	99.85	71.46	79.76	99.99	0.00	0.00	79.65	81.04	0.00	0.00
3.00	7.98E-5	0.22	0.22	0.45	1.4E-11	1.5E-11	0.12	99.97	56.37	65.41	100.00	0.00	0.00	65.39	67.27	0.00	0.00
4.00	2.59E-5	0.30	0.16	0.41	1.9E-12	3.0E-11	0.13	99.99	47.16	55.67	100.00	0.00	0.00	55.67	57.72	0.00	0.00

The effect of CO<sub>2</sub>/CH<sub>4</sub> feed ratio in the feed on CH<sub>4</sub> and CO<sub>2</sub> equilibrium conversions is also listed in Table 4 at 1123 K and 1 atm. Increasing CO<sub>2</sub>/CH<sub>4</sub> feed ratio enhances the CH<sub>4</sub> conversion and decreases the CO<sub>2</sub> conversions. However, the CH<sub>4</sub> conversion at CO<sub>2</sub>/CH<sub>4</sub> feed ratio higher than 1 is larger than the CO<sub>2</sub> conversion owing to the reaction between CO<sub>2</sub> gas in the feed and H<sub>2</sub> in the product. Smaller CH<sub>4</sub> conversion compared to CO<sub>2</sub> conversion at CO<sub>2</sub>/CH<sub>4</sub> feed ratio below 1 implies that the CO<sub>2</sub> acts as a limiting reactant as corroborated by the decreasing H<sub>2</sub> mole fractions at similar conditions. Considerable reduction in the CO<sub>2</sub> conversion is also exhibited in Table 4 at CO<sub>2</sub>/CH<sub>4</sub> feed ratio higher than 1, where CH<sub>4</sub> acts as the limiting reactant.

The predicted equilibrium selectivity for CH<sub>4</sub>-CO<sub>2</sub> reaction system is also presented in Table 4. Significant C<sub>2</sub>H<sub>6</sub> and C<sub>2</sub>H<sub>4</sub> equilibrium selectivities are achieved at lower CO<sub>2</sub> mole fraction in the feed and decrease considerably at higher CO<sub>2</sub>/CH<sub>4</sub> feed ratio. The results are in contrast to results for the catalytic CO<sub>2</sub> OCM reaction [17,18]. The difference may be attributed to the role of the catalyst in enhancing the selectivity toward the desired reaction at certain condition. Similar trend is also shown by CO and H<sub>2</sub> equilibrium selectivities where the selectivi-

ties are almost 100% at CO<sub>2</sub>/CH<sub>4</sub> feed ratio less than 1. However, the H<sub>2</sub> selectivity starts decreasing at CO<sub>2</sub>/CH<sub>4</sub> feed ratio more than 1 possibly caused by more H<sub>2</sub> converted to water and CO *via* Reaction (2), as demonstrated by larger CO and H<sub>2</sub>O mole fractions at the same conditions. C<sub>2</sub>H<sub>6</sub> and C<sub>2</sub>H<sub>4</sub> yields decline markedly with increasing CO<sub>2</sub>/CH<sub>4</sub> feed ratio. H<sub>2</sub> and CO yields are enhanced with CO<sub>2</sub>/CH<sub>4</sub> feed ratio, wherein the H<sub>2</sub> yield approaches the CO yield at CO<sub>2</sub>/CH<sub>4</sub> feed ratio 1. Consequently, increasing the CO<sub>2</sub>/CH<sub>4</sub> feed ratio above 1 decreases the H<sub>2</sub> and CO yields due to the decrements of H<sub>2</sub> selectivity and CO<sub>2</sub> conversion and the role of CH<sub>4</sub> as limiting reactant. The decrement of H<sub>2</sub> yield at CO<sub>2</sub>/CH<sub>4</sub> feed ratio more than 1 may be caused by favourable reaction of H<sub>2</sub> with CO<sub>2</sub> (Reaction (2)).

### 3.4. Effect of system pressure on equilibrium mole fraction, conversion, selectivity and yield

The influence of system pressure on the performance of reactions can be expressed by Equation (17) [15] as inline with LeChatelier's principles.

$$\prod_{i=1}^I (y_i)^{\nu_i} = \left( \frac{P}{P_o} \right)^{-\nu} K \quad (17)$$



If the total stoichiometric number  $\nu (\equiv \sum_i \nu_i)$  is negative, Equation (17) shows that an increase in  $P$  at constant  $T$  causes an increase in  $\prod_{i=1}^I (y_i)^{\nu_i}$  implying a shift of the reaction to the right (product) side. If  $\nu$  is positive, an increase in  $P$  at constant  $T$  leads to a decrease in  $\prod_{i=1}^I (y_i)^{\nu_i}$  exhibiting a shift of the reaction to the left (reactant) side. But, if  $\nu$  is zero, the change in system pressure does not influence the reaction direction.

Reactions (1) and (2) show a positive stoichiometric number ( $\nu$ ), in which increasing the system pressure decreases the mole fractions of both prod-

ucts at equilibrium as depicted in Figure 5(a). Similar trend also appears in Figure 6 corresponding to lower  $H_2$  and  $CO$  selectivities with system pressure. The interesting trend is exhibited by equilibrium mole fractions of ethane and ethylene as shown in Figure 5(b), which are presented for temperatures 923, 1123 and 1223 K. In fact, the equilibrium mole fractions of both products are enhanced slightly by increasing the system pressure. At temperature below 1123 K, for example low temperature (923 K),  $C_2H_6$  mole fraction is markedly higher than that of  $C_2H_4$ . In this case, other possible reactions may occur rather than dehydrogenation of ethane only which controls the trend as presented in Reactions (6) and (7) [19].

Reaction (6):  $C_2H_6 + CO_2 \rightleftharpoons C_2H_4 + CO + H_2O$

Reaction (7):  $C_2H_6 + 2CO_2 \rightleftharpoons 4CO + 3H_2$

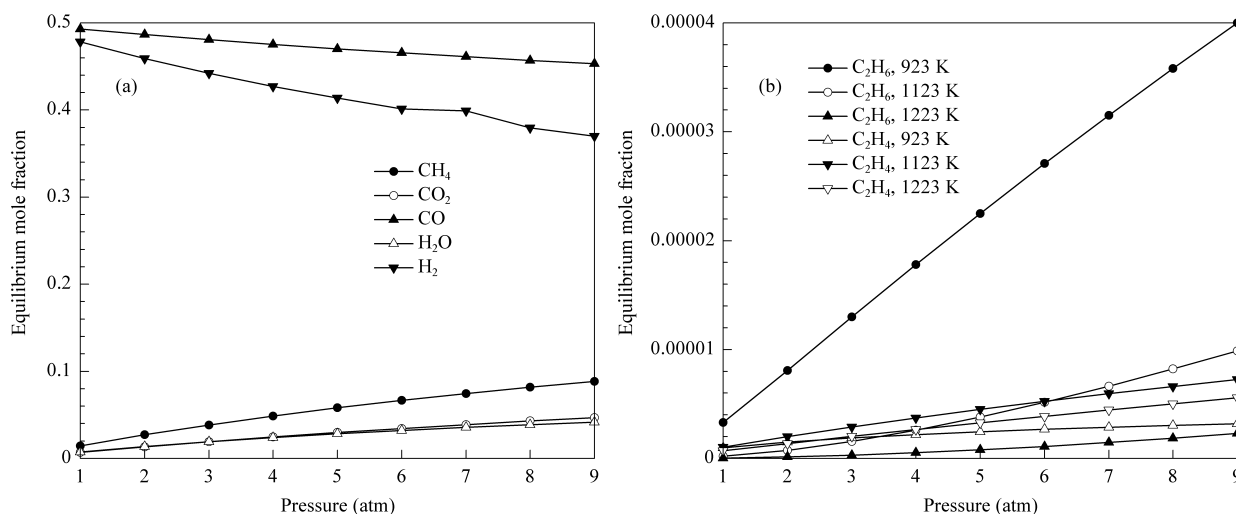


**Figure 5.** Effect of system pressure on equilibrium mole fractions of products at  $CO_2/CH_4$  feed ratio 1

(a)  $CH_4$ ,  $CO_2$ ,  $CO$ ,  $H_2O$  and  $H_2$  at temperature 1123 K, (b)  $C_2H_6$  and  $C_2H_4$  at temperature 923, 1123 and 1223 K

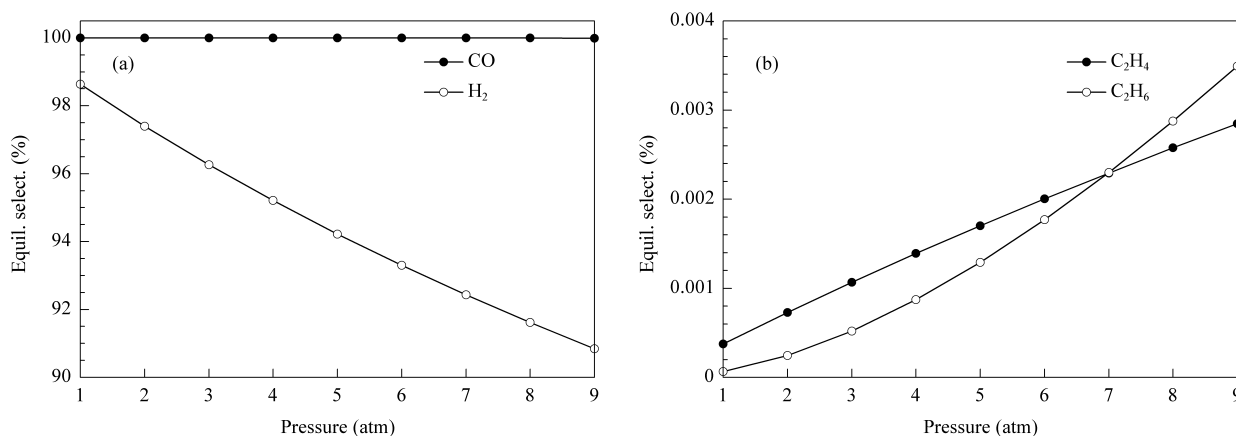


**Figure 6.** Effect of system pressure on equilibrium selectivities of  $H_2$ ,  $CO$ ,  $C_2H_6$  and  $C_2H_4$  products at temperature 1123 K and  $CO_2/CH_4$  feed ratio 1

Accordingly, by increasing the system pressure the reactions shift to the left side, which in turn enhances  $C_2H_6$  mole fraction and decrease  $C_2H_4$  mole fraction. The trend is also confirmed by the difference of  $\Delta G_T^\circ$  value for both  $CO_2$  OCM reactions (Reactions (3-4)). Based on Table 2, the  $\Delta G_T^\circ$  of Reaction (3) is lower than that of Reaction (4) at temperature lower than 1000 K. Thus, Reaction (3) is more favourable to produce  $C_2H_6$  than Reaction (4). But, the distinct trend is shown at temperature higher than 1123 K, in which the  $C_2H_4$  mole fraction tends to be more than the  $C_2H_6$ . The trend is linked to the standard Gibbs free energy change presented in Table 2, wherein at temperature higher than 1000 K the dehydrogenation reaction (Reaction (5)) is significantly favourable and also that  $\Delta G_T^\circ$  value for Reaction (4) is less than Reaction (3). It is also interesting to see the effect of pressure for temperature at 1123 K. As the pressure rises above 6 atm, the effect of system pressure is dominant towards the equilibrium and shifts the Reactions (6) and (7) to the left side, which in turn increases the  $C_2H_6$  mole fraction as compared to the  $C_2H_4$  mole fraction. Similar trend is demonstrated by the equilibrium selectivities for  $C_2H_6$  and  $C_2H_4$  as shown in Figure 6 for temperature at 1123 K.

The effect of system pressure on the equilibrium conversions of  $CH_4$  and  $CO_2$  at 1123 K and  $CO_2/CH_4$  feed ratio being 1 is exhibited in Figure 7. The equilibrium conversions of  $CH_4$  and  $CO_2$  decrease with

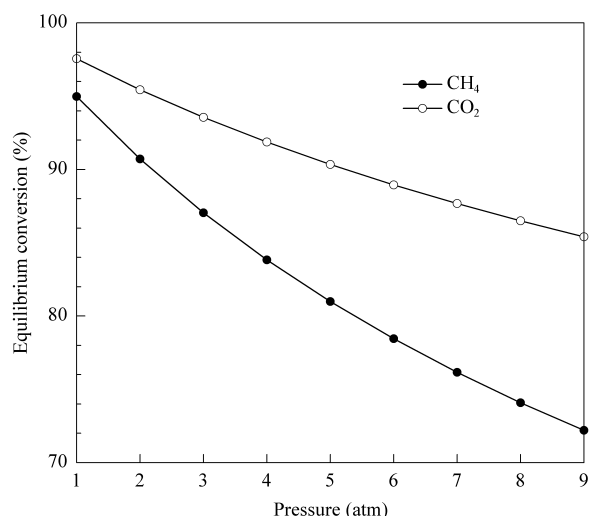


**Figure 7.** Effect of system pressure on equilibrium conversions of  $CH_4$  and  $CO_2$  at temperature 1123 K and  $CO_2/CH_4$  feed ratio 1

increasing system pressure. The reaction shifted to the reactant side and decreased the reaction coordinate due to positive and/or zero stoichiometric num-

ber ( $\nu$ ) of all reactions considered (Reactions (1)-(5)), which in turn decreases the  $\prod_{i=1}^I (y_i)^{\nu_i}$  term in Equation (17).

### 3.5. Effect of temperature and $CO_2/CH_4$ feed ratio on carbon and no carbon formation regions at equilibrium

In this section, carbon is added into the above chemical equilibrium system in order to study the conditions at which the carbon is formed. Pertaining to this system,  $CH_4$ ,  $CO_2$ ,  $CO$ ,  $H_2$ ,  $C_2H_4$ ,  $C_2H_6$ ,  $H_2O$  and  $C$  (carbon) exist in the equilibrium system. The  $CH_4$  and  $CO_2$  are stated as the reactants, while  $CO$ ,  $H_2$ ,  $C_2H_4$ ,  $C_2H_6$  and  $H_2O$  are defined as products. The range of conditions under which carbon will form in the equilibrium system is depicted in Figure 8. The curve was plotted by determining the points corresponding to the first disappearance of carbon as the temperature is increased for each fixed  $CO_2/CH_4$  feed ratio. From the figure, the area of carbon formation region is exhibited below the curve, while that of no carbon formation region is demonstrated above the curve. The carbon may be formed *via* methane decomposition and/or Boudouard reaction [20,21] as exhibited in Reactions (8) and (9), respectively.

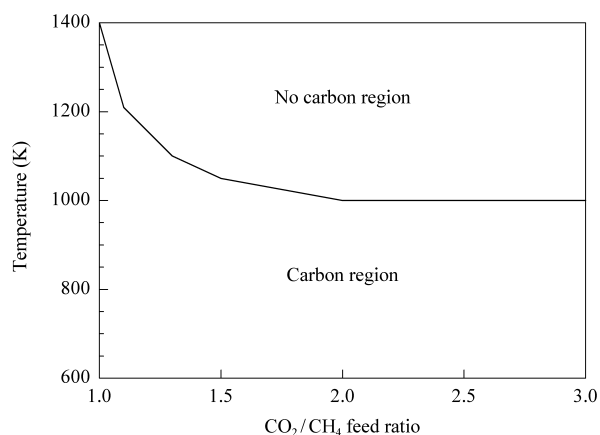
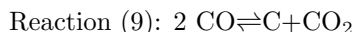


**Figure 8.** Carbon and no carbon formations region at 1 atm as function of temperature and  $CO_2/CH_4$  feed ratio

From Figure 8, it is found that carbon forms in the entire range of temperature at  $CO_2/CH_4$  feed ratio below 1. At  $CO_2/CH_4$  ratio above 1, the temperature limit for no carbon formation region decreases as the  $CO_2/CH_4$  ratio increases. It is shown that no

carbon formation region is only found at temperature higher than 1000 K and  $\text{CO}_2/\text{CH}_4$  ratio higher than 1. Through this figure, the operating conditions ranges of  $\text{CH}_4$  and  $\text{CO}_2$  reactions at which the carbon does not form at equilibrium can be recommended.

#### 4. Conclusions

The feasibility of all possible  $\text{CH}_4$  and  $\text{CO}_2$  reactions can be studied by thermodynamic chemical equilibrium using direct minimization of Gibbs free energy. The thermodynamic equilibrium analysis on the  $\text{CH}_4$  and  $\text{CO}_2$  reactions showed that Reaction (1), Reaction (2), and Reaction (5) were more favourable than  $\text{CO}_2$  OCM reaction (Reactions (3-4)) without catalyst. The  $\text{CO}_2/\text{CH}_4$  feed ratio, reaction temperature, and system pressure gave significant effect on the equilibrium composition, equilibrium conversion, selectivity and yield. It was found that  $\text{CO}_2/\text{CH}_4$  feed ratio of 1 is suitable for synthesis gases production with the  $\text{H}_2/\text{CO}$  ratio unity through Reaction (1) at temperature higher than 1100 K. Meanwhile, the  $\text{CH}_4$  and  $\text{CO}_2$  conversions and selectivity of synthesis gases decreased with increasing system pressure. From the thermodynamic chemical equilibrium studies and standard Gibbs free energy change ( $\Delta G_T^\circ$ ) analysis, it can be deduced that the  $\text{CO}_2$  OCM reaction (Reactions (3, 4)) was less favourable. However, the performance of the  $\text{CO}_2$  OCM reaction may be more favourable, but not impressive in the presence of a suitable catalyst. In addition, the range of operating conditions at equilibrium for the  $\text{CH}_4$  and  $\text{CO}_2$  reactions at which no carbon is formed can be recommended. Numerical results indicated that the no carbon formation region was at temperatures above 1000 K and  $\text{CO}_2/\text{CH}_4$  ratio larger than 1.

#### Acknowledgments

The authors would like to express their sincere gratitude to the Ministry of Science, Technology and

Innovation (MOSTI), Malaysia for the financial support received under the IRPA Project No 02-02-06-0016 EA099.

#### References

- [1] Suhartanto T, York A P E, Hanif A *et al.* *Catal Lett*, 2001, **71**: 49
- [2] Centi G, Cavani F, Trifirò F. *Selective Oxidation by Heterogeneous Catalysis*. New York: Kluwer Academic/Plenum Publishers, 2001
- [3] Chen G. *J Nat Gas Chem*, 2002, **11**: 109
- [4] Wang Y, Takahashi Y, Ohtsuka Y. *J Catal*, 1999, **186**: 160
- [5] Vasudeva K, Mitra N, Umasankar P *et al.* *Int J Hydrogen Energy*, 1996, **21**: 13
- [6] Chan S H, Wang H M. *Int J Hydrogen Energy*, 2000, **25**: 441
- [7] Lutz A E, Bradshaw R W, Keller J O *et al.* *Int J Hydrogen Energy*, 2003, **28**: 159
- [8] Lutz A E, Bradshaw R W, Bromberg L *et al.* *Int J Hydrogen Energy*, 2004, **29**: 809
- [9] Guéret C, Daroux M, Billaud F. *Chem Eng Sci*, 1997, **52**: 815
- [10] Lwin Y, Daud W R W, Mohamad A B *et al.* *Int J Hydrogen Energy*, 2000, **25**: 47
- [11] Tang H, Kitagawa K. *Chem Eng J*, 2005, **106**: 261
- [12] Douvartzides S L, Coutelieres F A, Demin A K *et al.* *AIChE J*, 2003, **49**: 248
- [13] Chan S H, Wang H M. *J Power Sources*, 2004, **126**: 8
- [14] Liu W Ch, Xu Y P, Tian Z J *et al.* *J Nat Gas Chem*, 2003, **12**: 237
- [15] Smith J M, Van Ness H C, Abbott M M. *Introduction to Chemical Engineering Thermodynamics*, New York: McGraw Hill Book, Co., 2001
- [16] Laosiripojana N, Assabumrungrat S. *Appl Catal B: Env*, 2005, **60**: 107
- [17] Wang Y, Takahashi Y, Ohtsuka Y. *J Catal*, 1999, **186**: 160
- [18] Wang Y, Ohtsuka Y. *Appl Catal A: Gen*, 2001, **219**: 183
- [19] Wang S, Zhu Z H. *Energy Fuels*, 2004, **18**: 1126
- [20] Froment G F. *J Mol Catal A: Chem*, 2000, **163**: 147
- [21] Ito M, Tagawa T, Goto S. *Appl Catal A: Gen*, 1999, **177**: 15